Check for updates

# Research on comprehensive assessment of coastal erosion intensity based on multi index method

Guowei Fu[1†], Mingguang He[1†], Xiaofeng Chen[2]*, Miao Fu[1]*,
Yanwei Song[1], Chenglong Wei[1], Hongbing Wang[1]
and Daheng Zhang[1]

[1]Haikou Marine Geological Survey Center, China Geological Survey, Haikou, China, [2]Hainan Honsheen Investigation & Design Co., LTD, Haikou, Hainan, China

The intensity of coastal erosion is a measure of the strength of erosion processes affecting coastal areas. Traditionally, assessments of coastal erosion intensity have relied on singular indices, such as the rate of shoreline retreat or erosion, often prioritizing higher rates over lower ones. This approach, however, lacks comprehensive consideration and scientific rigor. In this study, we adopt a more holistic approach by examining the Qionghai-Wanning coast on the eastern side of Hainan Island. We selected four indices that reflect local conditions and influence coastal erosion strength: Annual rate of shoreline change (T1), Beach annual down-cutting rate (T2), Beach slope (T3), Average particle size of the beach (T4). These indices were used to comprehensively evaluate the erosion intensity of the Qionghai-Wanning coast. The evaluation results categorized the study area into six grades: serious erosion (3.45%), strong erosion (6.90%), erosion (20.69%), micro erosion (44.38%), stabilization (20.69%), and accretion (3.45%). The findings indicate that, under the broader environmental trends of global warming and rising sea levels, most sandy coasts exhibit micro-erosion intensity. Areas experiencing strong and serious erosion are predominantly influenced by human activities, such as those occurring in promenade bays, artificial islands, and harbors. To further understand the relationship between these factors and erosion intensity, we employed the Spearman correlation coefficient method. The analysis revealed that the T1 and the T2 are the primary factors influencing coastal erosion intensity, with the T4 serving as a secondary factor. These factors collectively impact the force and energy absorption of the coast through wave and tidal actions, ultimately determining the intensity of coastal erosion. The multi-index assessment method for coastal erosion intensity demonstrated an accuracy of 82.75%, providing a scientific basis for the management, protection, and restoration of coastal areas.

# 1 Introduction

Against the backdrop of global warming, rapid sea-level rise, frequent extreme climate events, and intensified human production activities, coastal zones are suffering from increasingly severe coastal erosion disasters. This poses huge threats to coastal engineering, natural ecological shorelines, and ecosystems (Jabour, 2011; Shi and Kasperson, 2015). Coastal erosion is a dynamic process of coastal change characterized by a deficit due to the imbalance of sediment budget in a certain segment of the coast, This process is primarily evidenced by the retreat of the shoreline, the scouring and down-cutting of the beach surface, as well as the down-cutting of low tidal flats while high tidal flats remain stable, and the coarsening of sediments (Mangor, 2017; Marcel, 2012). In the field of coastal erosion science, research has expanded into various directions as a result of ongoing in-depth exploration. These directions include studying coastal erosion processes and mechanisms (Bruun, 1962; Chapman et al., 1982; Thampanya et al., 2006; Chen et al., 1988, 2004), analyzing erosion patterns and models (Feng et al., 2008; Feng, 2021), assessing erosion hazards (Boruff et al., 2005; Merlotto et al., 2016; Mohamed et al., 2021), evaluating coastal erosion vulnerability (Liu, 2015; Chao et al., 2022a; Chao et al., 2022b; Feng et al., 2022; Fu et al., 2022), and examining the quantitative relationship between erosion protection management and economic factors. Nonetheless (Bolle et al., 2021; Hagedoorn et al., 2021), there remains a notable gap in research efforts regarding the assessment of coastal erosion intensity.

The intensity of coastal erosion reflects the severe scouring and eroding of the coast, including the rate at which it recedes landward and undergoes down-cutting on the beach (Ma et al., 2017). The coast erosion intensity is not only related to the hydrodynamic conditions such as tides, waves, and typhoon storm surges, but also influenced by the comprehensive effects of local coastal geology, topography, and sand supply conditions along the coastal beaches (Feng, 2021). In the past, traditional assessments of coastal erosion intensity typically focused on isolated indicators such as the retreat rate of the shoreline, the down-cutting rate of the beach, and the rate of sediment coarsening on the beach surface for single-item evaluation. The principle of "choosing the higher value" was applied, with the most severe result of each individual evaluation value being used as the final assessment result of the intensity of coastal erosion disasters (Feng et al., 2019). It is important to note that the erosion intensity of different coastal sections varies significantly. Moreover, even within the same section, differences in erosion intensities can be observed at various locations, such as the subtidal zone, intertidal zone, and supratidal zone of the beach, due to variations in beach gradient, width, and grain size of sand and gravel. The single-factor assessment process often fails to fully capture the complexity and nuances of erosion intensity, as it lacks a comprehensive and in-depth research approach. For instance, in traditional evaluations of coastal erosion intensity based on the rate of change of the multi-year average high tide line or vegetation line, certain sections may exhibit no noticeable retreat in these lines. However, underlying changes such as significant beach down-cutting and alterations in grain size might go unnoticed, leading to an inaccurate characterization of the erosion as stable. This discrepancy between the assessment and the actual conditions primarily stems from a lack of holistic scientific analysis of the interconnectedness of various factors (Wen et al., 2017; Bazzichetto et al., 2020). For instance, an improved method for assessing coastal erosion intensity has been developed by Cao Chao (Chao, 2019). This method is based on the MABAC comprehensive algorithm and involves selecting ten evaluation indicators tailored to local conditions. To determine the weighting of these indicators, a combination of the decision experiment and evaluation method with the network AHP is employed to calculate subjective weights, while the CRITIC method is utilized to calculate objective weights. Subsequently, the improved MABAC method, which accounts for the short-board effect, is applied to conduct a comprehensive evaluation of coastal erosion intensity. This approach addresses the issue of subjective bias among evaluation indicator factors, enhances the flexibility of the expert judgment process, and ensures the rationality, credibility, and intuitiveness of the evaluation outcomes.

Additionally, some scholars When conducting coastal erosion research on the southern coast of Sri Lanka, Senevirathna et al. (2018) employed methods including field observations and questionnaire surveys with the community. They determined that stone-block paving is the primary factor accelerating erosion hazard in the area. In recent years, numerical simulation technologies like X-Beach and Delft3D have been extensively used in coastal erosion assessments to more accurately simulate the impact of storm surges and waves on the coast (Dano et al., 2009). Most use satellite images, GIS, and LiDAR technology to monitor long-term coastline changes and analyze erosion intensity. Different evaluation methods have advantages and disadvantages. Existing methods for assessing coastal erosion intensity have significant shortcomings. Firstly, assessments often rely on single-factor evaluations without fully considering the comprehensive impact of various factors on erosion intensity. Secondly, when using comprehensive indicators for evaluation, the assignment of indicator weights is often based solely on subjective or objective criteria, without fully integrating the benefits of both subjective and objective weights. Thirdly, while the uniqueness of evaluation results may appear accurate, it can actually violate the uncertainty and ambiguity of the physical meaning of specific evaluation objects, leading to biased evaluation results.

This study focuses on the Qionghai-Wanning coast in the eastern part of Hainan Island, using it as a case study to investigate coastal erosion. Four key index factors impacting the intensity of coastal erosion were selected: Annual rate of shoreline change (T1), Beach annual down-cutting rate (T2), Beach slope (T3), and Average particle size of the beach (T4). By employing the objective independence weight method to assess the weight of each factor index and utilizing the index data, the erosion intensity index (EII) for various evaluation units was calculated through weighting. This process allowed for the determination of the degree of coastal erosion and how it is influenced by a combination of factors. The study delves into an analysis of the primary and secondary factors that contribute to coastal erosion, facilitating the identification of the key controlling factors influencing erosion intensity. Ultimately, the research provides valuable scientific insights to support the strategic management of coastlines and the implementation of effective ecological restoration measures.

## 2 Materials and methods

### 2.1 Study area

Coastal erosion has become the most prominent disaster issue on the coast of Hainan Island, with the study area on the Qionghai-Wanning coast in the eastern part of the Hainan Island being severely affected. The study area is situated between 110°00' to 110°40'E and 18°35' to 19°29'N. In the 1970s and 1980s, around 53% of the coastline on Hainan Island was already affected by erosion (Xia et al., 1993). This figure increased to 71.9% by the 1990s. There are a total of 64 eroded coastlines on the island, with 7 sections experiencing strong erosion. Notably, 3 of these strongly eroded sections are located within the study area, representing approximately 42.8% of such instances on the island (Chen, 2010). Therefore, the varying degrees of erosion make Hainan Island an ideal location for assessing erosion intensity.
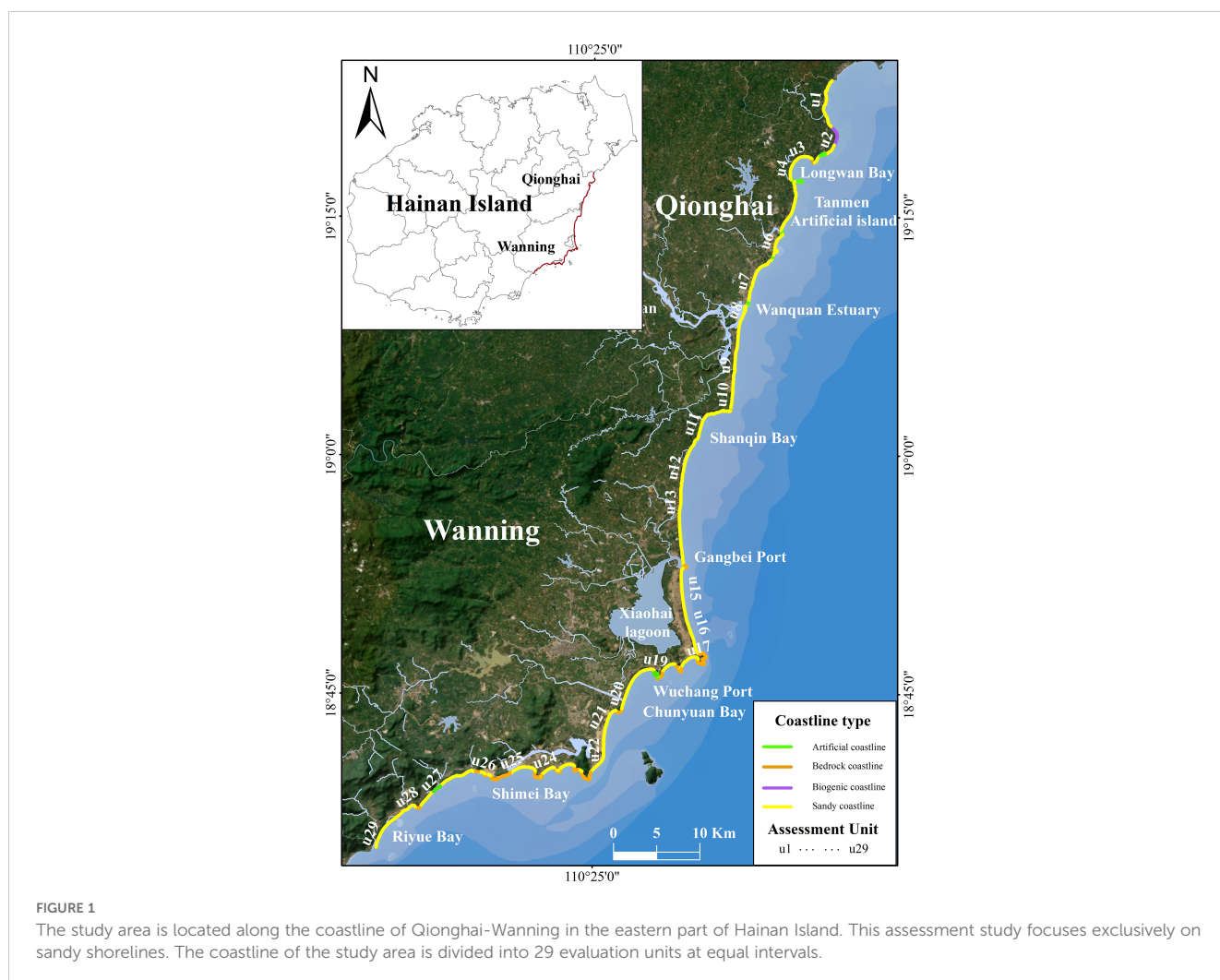
The continuous acceleration of coastal erosion on Hainan Island is mainly attributed to enhanced human activities. These activities include the construction of reservoirs in the upper reaches of rivers, sand excavation from riverbeds and coastlines, mining of coral reef beach rocks, and various coastal engineering projects.

These human actions, when combined, exert significant pressure on the coastline. Moreover, the coastal erosion is further compounded by the comprehensive effects of frequent typhoons and other harsh marine weather conditions that continuously scour the coast (Chen, 2010). Based on field survey measurements, the total length of the coastline studied is 153.73 kilometers. Of this total, the sandy coastline constitutes 117.86 kilometers, which accounts for 76.67% of the entire coastline. The remaining portion comprises a small amount of artificial coastline, bedrock coastline, and biogenic coastline. This assessment, however, focuses exclusively on the sandy coastline within the study area. This study divides the coastline of Qionghai-Wanning into 29 assessment units (u1-u29) according to the principle of equal interval spacing, and comprehensively assesses the stability of the coastline (Figure 1).

### 2.2 Indicator selection and data sources

#### 2.2.1 Indicator selection

The retreat rate of the coastline and the rate of beach down-cutting are the most commonly used indicators to characterize the intensity of erosion. A higher rate of beach down-cutting and coast



FIGURE 1
The study area is located along the coastline of Qionghai-Wanning in the eastern part of Hainan Island. This assessment study focuses exclusively on sandy shorelines. The coastline of the study area is divided into 29 evaluation units at equal intervals.

retreat is indicative of a more powerful wave scouring action, signaling a higher level of coastal erosion intensity. Conversely, lower rates of beach down-cutting and coast retreat suggest a weaker erosion intensity. The beach gradient and particle size play a crucial role in determining the wave reflection capacity, which directly impacts the strength of erosion, thereby influencing the characteristics of coastal erosion intensity. Specifically, a beach with a coarser sand layer and steeper surface exhibits a greater reflective action of waves, leading to increased waves' ability to suspend and roll sediment and consequently resulting in higher erosion intensity by waves on the beach. Thus, beach slope and particle size are vital factors that influence the intensity of coastal erosion and scouring.

In this study, four indicators reflecting the intensity of coastal erosion were comprehensively selected based on the coastal characteristics of the study area and in adherence to the principles of systematization, scientificity, authenticity, objectivity, and operability. These indicators include the Annual rate of shoreline change (T1), Beach annual down-cutting rate (T2), Beach slope (T3) and Average particle size of the beach (T4), chosen according to local conditions for a weighted comprehensive assessment.

## 2.2.2 Data sources

The data sources for the indicators primarily involve collecting data through various methods such as field surveys of erosion and accretion, beach profile monitoring, and remote sensing interpretation. Among these methods, T1 utilizes Google Earth

satellite imagery, maintaining consistent resolution and seasonal conditions. The selected imagery spans seven time periods: 1985, 1990, 1995, 2000, 2005, 2010, and 2015 (Figure 2), all with a resolution of 16.8 meters. To extract the coastline for each year, the method of visual interpretation was employed, using the high tide line as the reference standard. The Lineament Raster Routing (LRR) method, provided by the Digital Shoreline Analysis System (DSAS) version 4.3 (http://woodshole.er.usgs.gov/project-pages/dsas/), is applied to quantify the coastline changes observed within each evaluation unit (Deepika et al., 2013).

The T2 data is derived from monitoring 44 beach profiles located in the Qionghai-Wanning coastal zone on the eastern side of Hainan Island (Figure 2). This inter-annual monitoring allows for the calculation of the erosion and sedimentation rates for each beach. This is based on the interannual average erosion and accretion changes of the beaches, measured in centimeters per year (cm/a), where a positive value denotes beach accretion and a negative value denotes beach regression.

The T3 data were obtained from 111 field survey measurement points in the study area, collected in 2021 (Figure 2). In cases where multiple survey points exist within a single evaluation unit, the average bank slope from those points is used to represent the slope value for that section., measured in degrees (°).

T4 collected sand samples from the supratidal, intertidal, and subtidal zones of 44 beach profiles for particle size analysis. A total of 132 data points were gathered for testing. The average particle
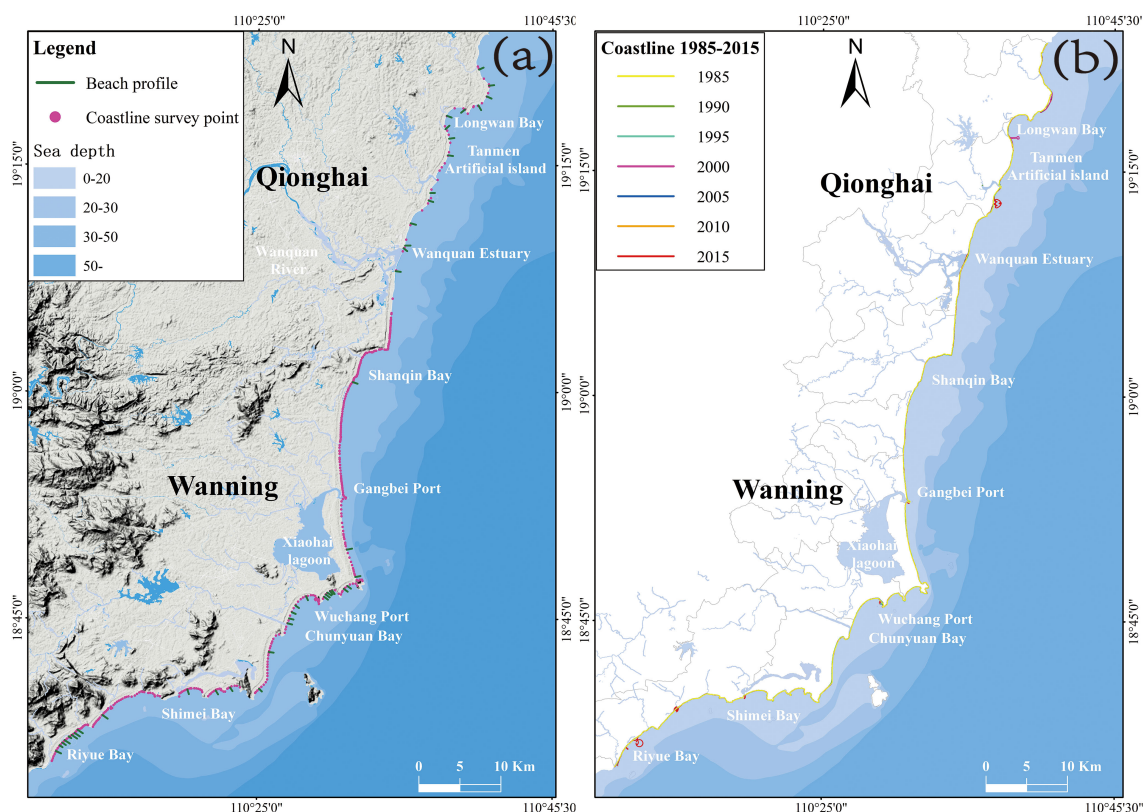
size of each section is taken as the result, and the unit is millimeters (mm).

### 2.2.3 Data processing

Based on the extraction of raw data, since the units and numerical magnitudes of different factor indicators' sample data vary and have different orientations on the actual strength of the coast, with both positive and negative values, in order to make the data applicable for comprehensive evaluation and ensure comparability between sample data of various factor indicators for the purpose of comprehensive assessment, we refer to Cai Feng's (2019) method for assessing coastal erosion vulnerability and apply normalization to the raw data.

In the process, we normalize the minimum value ($min\{u_{ij}\}$) of each indicator's data to 0.5 and the maximum value ($max\{u_{ij}\}$) to 4.5. It is important to note that different indicators have distinct normalization formulas. Specifically, when the sample data of the factor indicator positively influences the intensity of coastal erosion, we apply formula 1. Conversely, if the sample data of the factor indicator negatively impacts the intensity of coastal erosion, we utilize formula 2. Consequently, the normalized values of each indicator are detailed in Table 1.

$$e_{ij} = \left[ \frac{u_{ij} - \min\{u_{ij}\}}{\max\{u_{ij}\} - \min\{u_{ij}\}} \right] \times 4 + 0.5 \qquad (1)$$

$$e_{ij} = 4.5 - \left[ \frac{\max\{u_{ij}\} - u_{ij}}{\max\{u_{ij}\} - \min\{u_{ij}\}} \right] \times 4 \qquad (2)$$

## 2.3 Evaluation method

### 2.3.1 Indicator weight division

The impact degrees of various indicators on the intensity of coastal erosion are different, which requires us to allocate the weights for each indicator. There are many methods in mathematical statistics for analyzing indicator weights, including Analytic Hierarchy Process (AHP) (Mosadeghi et al., 2015; Cabrera and Lee, 2019; Saffaria et al., 2020), entropy weight method (Cabrera and Lee, 2020), independent weight method (Shuying et al., 2018), etc. The choice of method should be based on the specific relationship between indicators and the evaluation requirements.

An objective weighting method known as the method of independent weight is employed in this study. This method determines weights based on the strength of collinearity between indicators (Shuying et al., 2018). When an indicator exhibits a strong correlation with other indicators, it suggests a significant overlap of information, thus indicating a lower weight assigned to this particular indicator. Conversely, if an indicator shows a weak correlation with other indicators, it implies that the indicator carries a substantial amount of unique information, warranting a higher weight allocation (Zhou and Ma, 2024). Its calculation method is to use the complex correlation coefficient R value obtained from regression analysis to represent the strength of collinearity (i.e., the strength of correlation).

The larger this value, the stronger the collinearity, and the lower the weight. The formula for R value is shown in formula 3. When calculating the weight, first, the reciprocal of the complex correlation coefficient R value, namely 1/R, is obtained, and then the value is normalized to obtain the weight. In this assessment, the four indicators of Annual rate of shoreline change (T1), Beach annual down-cutting rate (T2), Beach slope (T3), Average particle size of the beach (T4) have certain correlation in terms of causes, so we adopt the method of independence weight in this assessment.

$$R = \frac{\sum (x - \bar{x})(\hat{x} - \bar{x})}{\sqrt{\sum (x - \bar{x})^2 \sum (\hat{x} - \bar{x})^2}} \qquad (3)$$

The weights of the three indicators were calculated using SPSS (The SPSSAU Project, 2024) software (https://www.spssau.com), as shown in Table 2.

### 2.3.2 EII

After normalizing the numerical values, we made the comprehensive evaluation targets of each indicator comparable. The weight values of each indicator were obtained using the independence weight method. Subsequently, we conducted a weighted comprehensive calculation to derive the EII (Erosion Intensity Index) value. This index value serves as a measure of erosion intensity, with higher values indicating stronger erosion intensity and lower values representing weaker intensity. Following the grading standards for coastal erosion disasters (Feng and Xia, 2003), the EII values were classified into six levels of coastal erosion intensity: accretion, stabilization, micro erosion, erosion, strong erosion, and serious erosion. Ultimately, the erosion intensity of each coastal segment within the study area was conclusively determined.

# 3 Results

Based on the numerical range, we divided the comprehensive erosion intensity index (EII) values obtained into six equal parts, with the minimum value being 1.23 and the maximum value 3.33, resulting in an average interval of 0.35. The numerical ranges for each erosion intensity level have been detailed in Table 3, whereas Table 4 presents the EII values and corresponding erosion intensities for each evaluation segment. Subsequently, a distribution map illustrating erosion disaster intensity grades from Qionghai to Wanning was generated based on the various erosion intensities, as depicted in Figure 3.

## 3.1 Serious erosion

In a specific segment comprising only 3.45% of the Qionghai-Wanning coast, serious erosion is observed, predominantly at Qionghai Longwan Port (u4). This stretch of coast is a typical cape and bay coast, and an artificial island has been constructed there. The intensity of erosion in this area is closely associated with the robust hydrodynamic conditions present. These hydrodynamic conditions are primarily influenced by the geomorphology of the

TABLE 1   Statistical table of normalized treatment for index values.

| Assessment Unit | The Annual rate of shoreline change (T1) | Beach annual down-cutting rate (T2) | Beach slope (T3) | Average particle size of the beach (T4) |
|---|---|---|---|---|
| u1 | 1.76 | 2.54 | 0.50 | 4.16 |
| u2 | 2.87 | 4.50 | 1.52 | 2.17 |
| u3 | 1.71 | 2.94 | 1.63 | 3.74 |
| u4 | 4.50 | 2.94 | 1.28 | 4.49 |
| u5 | 0.50 | 1.08 | 2.87 | 2.35 |
| u6 | 1.79 | 2.87 | 1.21 | 4.37 |
| u7 | 1.64 | 1.07 | 2.04 | 3.94 |
| u8 | 1.16 | 0.50 | 2.04 | 1.40 |
| u9 | 1.65 | 1.70 | 0.97 | 2.19 |
| u10 | 1.68 | 1.70 | 2.41 | 2.19 |
| u11 | 1.64 | 2.38 | 3.03 | 2.19 |
| u12 | 1.65 | 2.38 | 2.72 | 2.19 |
| u13 | 1.73 | 2.38 | 2.54 | 2.19 |
| u14 | 1.72 | 2.07 | 4.50 | 0.50 |
| u15 | 1.55 | 2.07 | 2.32 | 0.50 |
| u16 | 1.63 | 1.87 | 2.56 | 0.50 |
| u17 | 1.53 | 2.27 | 1.69 | 0.93 |
| u18 | 1.56 | 1.36 | 2.31 | 2.51 |
| u19 | 1.80 | 3.59 | 2.83 | 3.72 |
| u20 | 1.64 | 4.15 | 1.77 | 1.46 |
| u21 | 1.74 | 4.15 | 0.97 | 3.42 |
| u22 | 1.78 | 1.97 | 1.05 | 3.40 |
| u23 | 1.56 | 2.58 | 1.77 | 3.83 |
| u24 | 1.67 | 2.58 | 1.29 | 3.48 |
| u25 | 1.62 | 1.82 | 1.09 | 3.51 |
| u26 | 1.59 | 2.27 | 2.40 | 3.64 |
| u27 | 1.70 | 2.27 | 1.53 | 3.64 |
| u28 | 1.61 | 2.26 | 3.15 | 2.17 |
| u29 | 2.14 | 0.89 | 2.95 | 3.35 |

TABLE 2   Calculate the weight values of each indicator through the independent weight method.

| Evaluation index | R | 1/R | Weight |
|---|---|---|---|
| Annual rate of shoreline change (T1)(m/a); | 0.470 | 2.129 | 26.61% |
| Beach annual down-cutting rate (T2) (cm/a) | 0.446 | 2.244 | 28.05% |
| Beach slope (T3) (°) | 0.550 | 1.819 | 22.74% |
| Average particle size of the beach (T4) (mm) | 0.553 | 1.808 | 22.60% |

R, Multiple correlation coefficient; 1/R : Reciprocal of the multiple correlation coefficient.

cape and bay coast as well as the presence of the artificial island. Notably, as waves approach the intricate formations of the cape and artificial island, refraction phenomena occur, leading to the concentration of wave energy along the cape's edges, as well as the north and south sides of the artificial island. Consequently, a scouring area with intense hydrodynamic activity is formed, surpassing the erosion effects observed in straight coastlines (Bu, 2021). This heightened erosion susceptibility is further compounded over time by extreme weather events such as typhoons and storm surges, culminating in the escalation of erosion intensity to a severe level within this particular segment.

TABLE 3   The interval values for each level of erosion intensity.

| level | Accretion | Stabilization | Micro Erosion | Erosion | Strong Erosion | Serious Erosion |
|---|---|---|---|---|---|---|
| Interval value | 1.23~1.58 | 1.59~1.94 | 1.95~2.30 | 2.31~2.66 | 2.67~3.02 | 3.03~3.38 |

## 3.2 Strong erosion

In the eastern part of Hainan, there are two sections, Qingge Port (u2) and Wanning Wuchang Port section (u19), with strong erosion grades, accounting for 6.9% of the study area coastline sections (Figure 3). The common feature of strong erosion in these

TABLE 4   Scale of coastal erosion intensity in the study area.

| Assessment Unit | EII | Erosion intensity | Notes |
|---|---|---|---|
| u1 | 2.23 | micro erosion | Shalao Estuary |
| u2 | 2.86 | strong erosion | Qingge Bay |
| u3 | 2.49 | erosion | |
| u4 | 3.33 | serious erosion | Longwan Bay, Tanmen Artificial island |
| u5 | 1.62 | stabilization | Tanmen Coral reef |
| u6 | 2.54 | erosion | Boao Artificial island |
| u7 | 2.09 | micro erosion | |
| u8 | 1.23 | accretion | Wanquan Estuary |
| u9 | 1.63 | stabilization | |
| u10 | 1.97 | micro erosion | Shanqin Bay |
| u11 | 2.29 | micro erosion | |
| u12 | 2.22 | micro erosion | |
| u13 | 2.20 | micro erosion | |
| u14 | 2.17 | micro erosion | Gangbei Port |
| u15 | 1.63 | stabilization | |
| u16 | 1.65 | stabilization | |
| u17 | 1.64 | stabilization | Bedrock shoreline |
| u18 | 1.89 | stabilization | Baoding Bay |
| u19 | 2.97 | strong erosion | Wuchang Port |
| u20 | 2.33 | erosion | Chunyuan Bay |
| u21 | 2.62 | erosion | |
| u22 | 2.03 | micro Erosion | |
| u23 | 2.41 | erosion | |
| u24 | 2.25 | micro erosion | Shimei Bay |
| u25 | 1.99 | micro erosion | Laoyehai Estuary |
| u26 | 2.43 | erosion | |
| u27 | 2.26 | micro erosion | |
| u28 | 2.27 | micro erosion | Riyue Bay |
| u29 | 2.25 | micro erosion | Riyue Artificial island |

areas is that it predominantly occurs in the nearshore sections adjacent to the ports. Qingge Port and Wuchang Port are significant fishing ports in the region, with Wuchang Port being classified as a first-class fishing port in Hainan. These open-type port have breakwaters that extend seaward, altering the direction of wave movement. The combination of frequent ship navigation and human activities in the vicinity contributes to the complexity of nearshore hydrodynamics, resulting in scouring along the adjacent coastline and leading to the occurrence of strong erosion.

## 3.3 Erosion

The distribution of coastal erosion intensity in the Qionghai-Wanning coastal area involves six sections, which collectively account for 20.69% of the total coastline. These sections are situated at various locations: Qionghai Longwan in the north, Boao Artificial Island, Wanning Chunyuan Bay, Longgun Estuary, Shime Bay, and other areas (Figure 3). The erosion mainly occurs in the coastal geomorphic areas of capes and artificial islands. Unlike serious erosion, the intensity of erosion primarily happens in the inner bay sections of capes, which often have soft beaches and gentle beach slopes. The hydrodynamic conditions in these inner bay sections are simpler than at the cape corners, and the intensity of erosion is relatively weak. A notable contrast is evident between Boao Artificial Island and Tamen Artificial Island, with the latter experiencing more severe erosion. Tamen Artificial Island is strategically located at the junction of a cape and a bay, introducing a higher level of hydrodynamic complexity due to the interaction between the cape and the artificial island. Consequently, the erosion intensity on Boao Artificial Island is less pronounced in comparison to Tamen Artificial Island, reflecting the impact of differing geographical configurations on erosion patterns.

## 3.4 Micro erosion

Micro-erosion occurs in a total of 13 sections, accounting for the largest proportion in the study area, reaching 44.83%. It is distributed along most of the coastline, mainly in locations such as the Shalao River in Qionghai, Boao Bay, Wanning's Shanqin Bay, and Riyue Bay (Figure 3). The main types of sections affected are estuarine near-shore sections, large bays, and straight soft beach sections. Micro-erosion is a widespread phenomenon that exists under the overall trend of global climate warming and sea level rise, exacerbated by frequent extreme weather events such as typhoon storm surges. Most soft sandy coastlines experience erosion. This micro-erosion will gradually reach a balanced state over a certain period of time, and under normal weather conditions, it will gradually become stable.
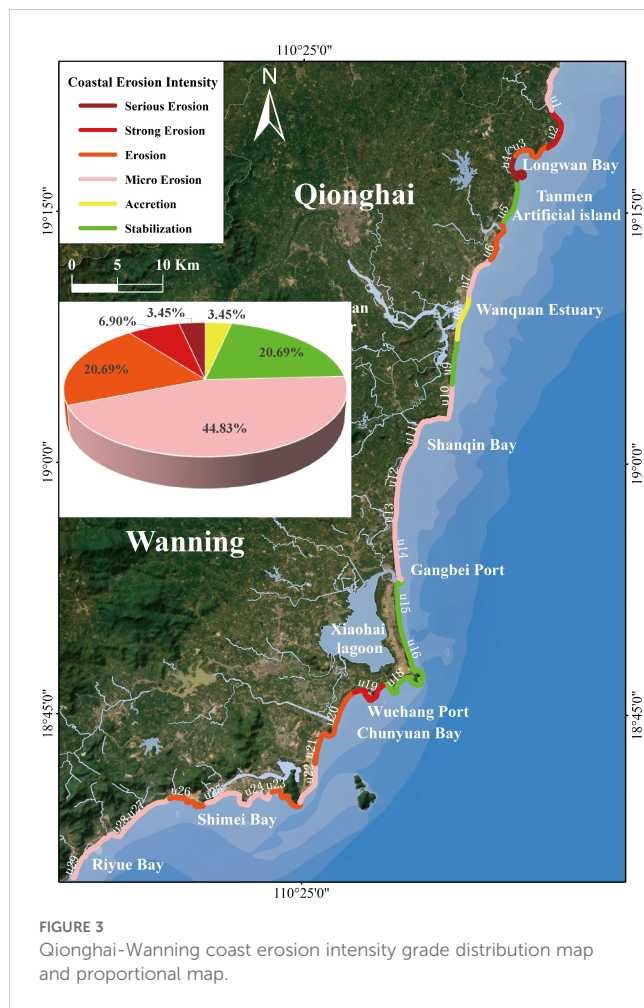
FIGURE 3
Qionghai-Wanning coast erosion intensity grade distribution map and proportional map.

## 3.5 Stabilization and accretion

The stable state in Qionghai-Wanning accounts for 20.69%, while the silted sections account for 3.45%. Stability is mainly distributed along the coastlines of Tamen in Qionghai, the Wanquan River estuary, and the southern entrance of the Xiao Hai lagoon in Wanning (Figure 3); the location of Qionghai Tamen is primarily stable because it has a large area of coral reef platforms near the shore, which weaken the waves to some extent. The reef flat length, surface roughness, and reef crown within the coral reef geomorphology directly relate to the deformation of wave propagation and act as a natural shoreline protection barrier (Shao, 2016). At the same time, the harder beach rock in some sandy beaches can further attenuate wave energy as it moves towards the shore, thus protecting the beach. Therefore, this section exhibits a stable state. The accretion sections are only distributed at the Wanquan River estuary in Qionghai. As the third-largest river in Hainan, the Wanquan River provides a stable source of sand for the shoreline through its annual sediment transport. Coupled with the erosion and scouring from the adjacent shoreline sections, the sediments are aggregated at the estuary entrance by the action of along-coast currents and other water flow, forming a silted floodplain at the mouth.

## 4 Discussion
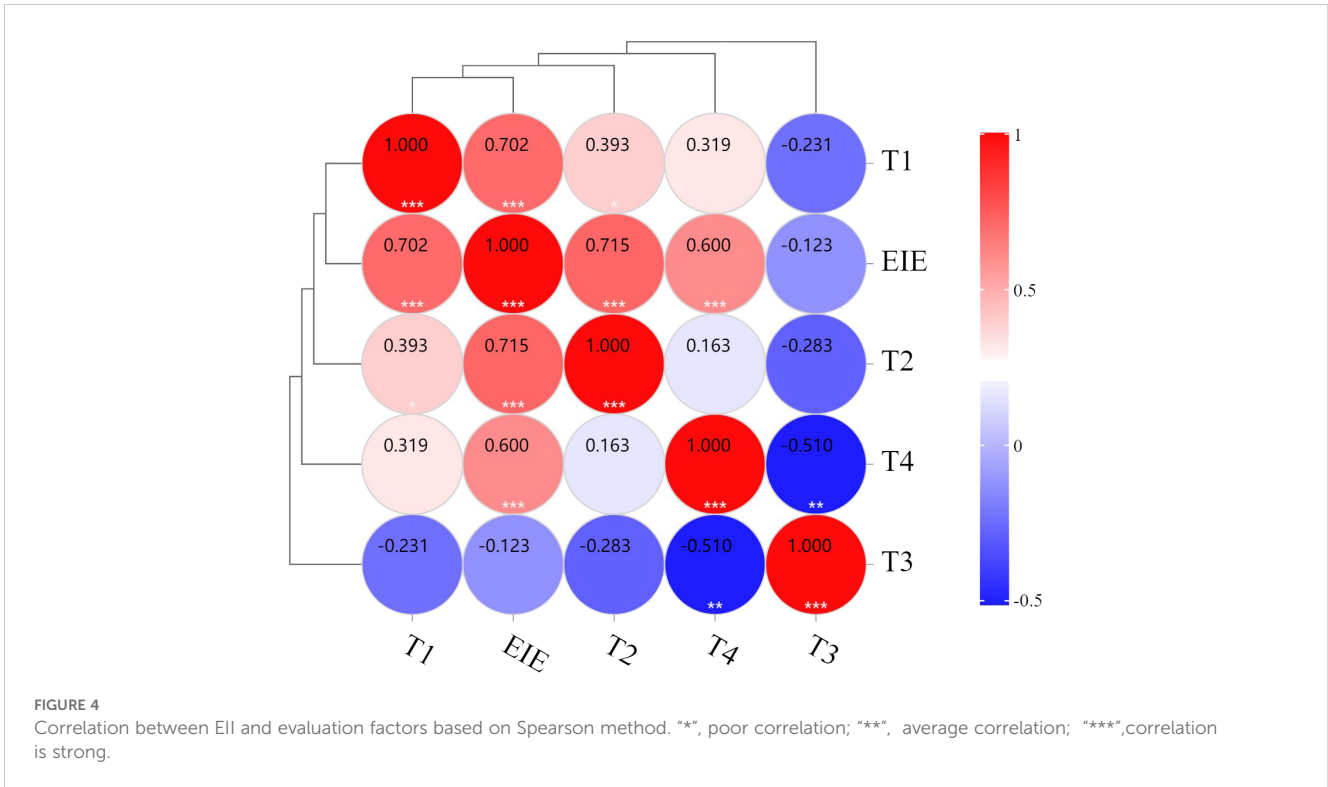
### 4.1 Erosion intensity influencing factor

We used the Spearson correlation coefficient method (Rodgers and Nicewander, 1988) to statistically analyze the relationship between the coastal erosion intensity in the study area and various indicator factors. By examining the correlation between each factor and the erosion intensity index, we aimed to identify the main controlling factors affecting coastal erosion intensity. The results of this analysis can be found in Figure 4.

The analysis revealed a significant linear relationship between the annual rate of shoreline change (T1), beach annual down-cutting rate (T2), average particle size of the beach (T4), and the coastal erosion intensity index (EII), as illustrated in Figure 5. The beach annual down-cutting rate (T2) exhibited the strongest correlation with the coastal erosion intensity index (r=0.717, p<0.01), indicating that higher annual intertidal erosion rates corresponded to increased coastal erosion intensity. Following closely, the annual rate of shoreline change (T1) was the second most correlated factor with the coastal erosion intensity index (r=0.702, p<0.01), demonstrating a strong relationship comparable to that of the beach annual down-cutting rate (T2). This suggests that both the annual rate of shoreline change (T1) and the beach annual down-cutting rate (T2) have similar impacts on coastal erosion intensity. In contrast, the average particle size of the beach (T4) exhibited a relatively weaker influence on the coastal erosion intensity index (EII). Notably, the beach slope (T3) did not display a linear relationship with the coastal erosion intensity index and did not exert a significant influence on coastal erosion intensity. Consequently, the annual rate of shoreline change (T1) and the beach annual down-cutting rate (T2) emerged as the principal determinants affecting coastal erosion intensity, while the average particle size of the beach (T4) was identified as a secondary factor in this context.

### 4.2 Comprehensive analysis of the impact of multiple factors on coastal erosion intensity

Traditionally, beach annual down-cutting rate and shoreline change rates have been employed as direct indicators of coastal erosion intensity. While this method is not inherently flawed, it does suffer from scientific limitations due to its lack of comprehensive consideration of the coastal environment. Often, there are less visible features that indirectly signify the characteristics of coastal erosion intensity. Among these are the slope and grain size of the beach, which are critical yet frequently overlooked factors. These elements interact with one another, influencing the impact and energy absorption of waves and tides on the coast. Consequently, they collectively determine the intensity of coastal erosion (Tim et al., 2011).

Beach slope significantly influences the energy distribution and direction of flows such as waves and tides. Steep beach slopes

FIGURE 4
Correlation between EII and evaluation factors based on Spearson method. "*", poor correlation; "**", average correlation; "***",correlation is strong.

increase the degree of wave breaking, accelerating the impact of water flow on the beach and thereby enhancing coastal erosion. Conversely, gentle slopes mitigate the impact of waves, alleviating coastal erosion (Dionísio et al., 2023). Additionally, beach sediment size plays a crucial role in coastal stability (Shi et al., 2007). Fine-grained beaches, characterized by compacted porosity due to water flow, can absorb more wave energy, thereby reducing the impact on the coast. In contrast, coarse-grained beaches, with larger pores, are less effective at absorbing wave energy, making the coast more

susceptible to erosion (McFall, 2019; Elsayed and Oumeraci, 2017). When considering both factors together, the combination of beach slope and sediment size affects the transmission of wave energy and the transport of sediments, ultimately influencing the intensity of coastal erosion (Dionísio et al., 2023). For instance, a steep, coarse-grained sandy beach will experience rapid erosion under strong wind and wave conditions, while a gentle, muddy beach will erode relatively slowly (Nans et al., 2019). In the study area, segments U7 and U8 have the same slope but differ in grain size, with U7 being



FIGURE 5
Linear regression chart of erosion intensity index and single factor index.
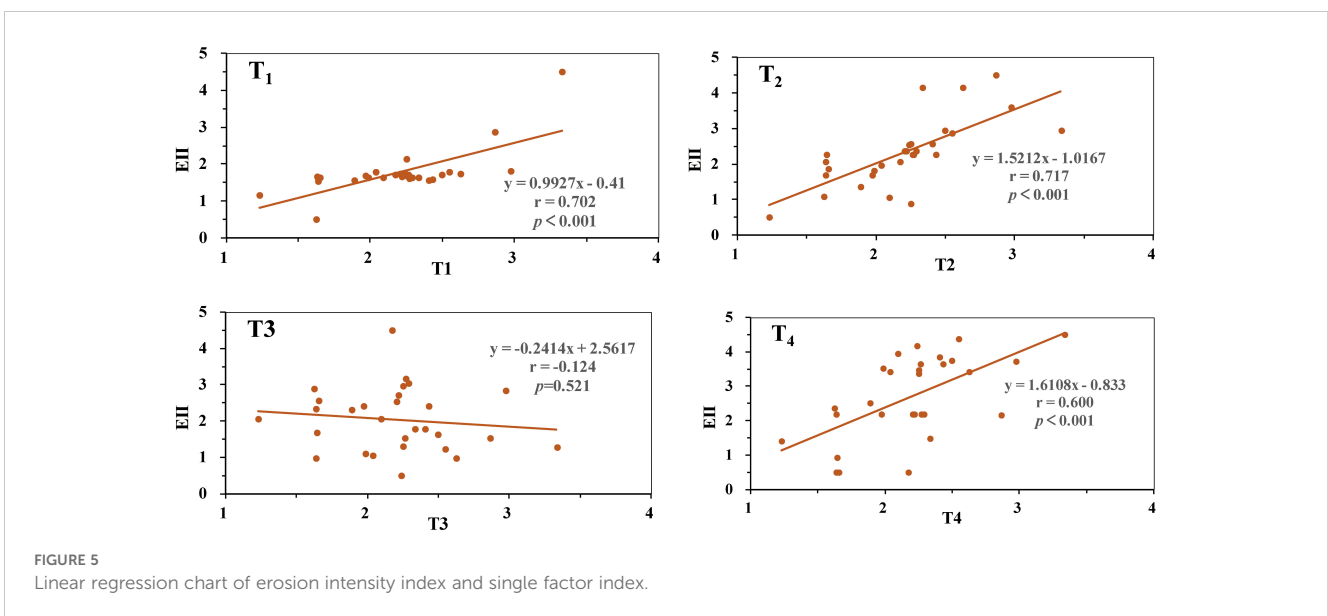
coarser and showing slight erosion, while U8 is finer and accumulating sediment. Similarly, when the average grain size is equal between U26 and U27, the higher slope of U26 leads to erosion, while U27 shows only micro-erosion.

The beach down-cutting rate reflects the speed at which beach material is carried away by water currents. A high beach down-cutting rate indicates rapid loss of beach material, suggesting a higher intensity of coastal erosion. The shoreline retreat rate, which measures the speed at which the coastline recedes, is a direct manifestation of the erosion process; the greater the retreat, the greater the erosion intensity (Bozzeda et al., 2023). The width and slope of the beach further influence both the beach sediment transport rate and the shoreline retreat rate. When the beach is wide and the slope is gentle, the energy of the waves dissipates as they approach the shore, weakening wave erosion and resulting in a lower sediment transport rate, thereby indicating weaker erosion intensity (Dionísio et al., 2023; Enríquez et al., 2019). In contrast, a narrow beach provides limited space for wave energy dispersion, and insufficient sediment accumulation reduces natural defenses against wave erosion, making it easier for the waves to erode the shoreline. The continuous increase in beach down-cutting rate leads to an increase in the shoreline change rate, as erosion gradually transitions to shoreline retreat, affecting the morphology and structure of the coast (Cigdem et al., 2020). Therefore, a high beach down-cutting rate, high shoreline retreat rate, steep beach slope, and coarse-grained beaches all exacerbate coastal erosion. Conversely, a low sediment transport rate, low shoreline retreat rate, gentle beach slope, and fine-grained beaches help mitigate the extent of coastal erosion.

## 4.3 Erosion intensity verification

To validate the reasonableness, authenticity, and scientific basis of the evaluation results, field surveys were undertaken in erosion coasts. During this validation process, the accuracy of the assessment results for different erosion intensities on each coast was determined based on evidence of coast erosion observed during the field surveys. Conversely, assessments categorized as silting or stable were deemed accurate if the field surveys corroborated the presence of silting or stability. Classifying erosion intensity in the field in a reasonable and scientific manner proved to be unfeasible, highlighting the importance of relying on the field surveys to validate the assessment results.

In the study area, a total of 37 erosion sections and 5 accretion sections were identified through field surveys, with the remaining areas classified as stable. The spatial distribution of erosion and accretion was visualized in Figure 6. A validation method was employed to assess the accuracy of the multi-index coast erosion intensity assessment. Out of the total 29 sections evaluated, 24 were correctly assessed, while 5 sections exhibited discrepancies. This resulted in an accuracy rate of 82.75% for the assessment method. During the field survey, the serious erosion area, Qionghai Longwan Port (u4), displayed significant damage, including destroyed buildings, toppled trees, and erosion scarps. Other sections with strong erosion, Qingge Port segment (u2) and Wanning Wuchang Port segment (u19), also showed coastal building damage. The Boao Artificial Island segment (u6) demonstrated retreating shorelines and erosion scarps, confirming the accuracy and scientific rigor of the assessment.

## 4.4 Limitations of evaluation methods

Through this study, it is found that there are three limitations: different time scales, difficulty of data acquisition and neglect of other environmental factors. First of all, the different time scales are reflected in the differences in the time scales obtained by the four indicators. For instance, the beach annual down-cutting rate may be affected by short-term storm surges, typhoons and other extreme events, but may not necessarily reflect the long-term average situation. Similarly The width and slope of the beach are also based on the data obtained in a short period of time, which is different from the time scale of other index data. Secondly, data acquisition poses significant challenges, requiring extensive beach surveys, measurements, and monitoring. This process is time-consuming and labor-intensive, hindering the widespread adoption and application of this evaluation system. Lastly, large-scale and national coastal erosion assessments often overlook other critical environmental factors, such as waves, tides, ocean currents, human activities, and geological structures. The exclusion of these factors from the assessment system compromises the scientific accuracy of the evaluation results.

Coastal erosion has been extensively studied in numerous countries worldwide, revealing various causes for changes in coastlines. In China, significant alterations in the coastline have occurred from 1991 to 2015, driven by both natural factors, such as climate change and storm surges, and human activities, particularly reclamation projects (Nan and Gong, 2018). The implementation of numerous coastal land reclamation projects, aimed at alleviating the shortage of coastal land resources, has markedly transformed China's coastline, especially since the 21st century (Shuai et al., 2021). Despite these substantial changes, research has predominantly focused on the alterations of the coastline, with comprehensive studies on the intensity of coastal erosion remaining particularly scarce. As science and technology continue to advance, it is imperative to evaluate the intensity of coastal erosion more scientifically. Furthermore, ongoing comprehensive studies are necessary to explore the relationship between various coastal environments and their impacts on the coastline. Such research is of great significance for the advancement of coastal scientific research, protection, restoration, and scientific management.

## 5 Conclusion

Building on previous research, this study takes the Qionghai-Wanning coast in the eastern part of Hainan Island as an example and selects four indicator factors that influence the intensity of coastal erosion: Annual rate of shoreline change (T1), Beach annual down-cutting rate (T2), Beach slope (T3) and Average particle size
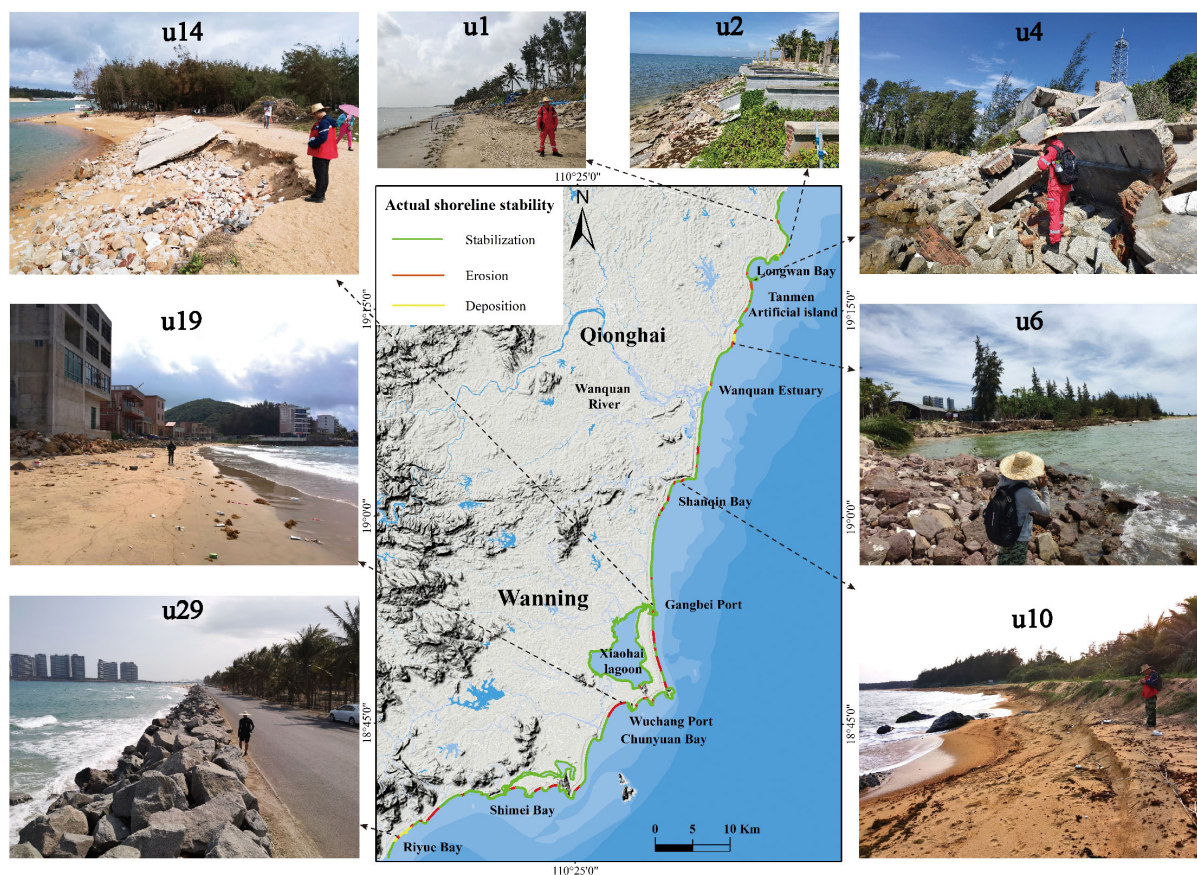
**FIGURE 6**
The actual survey of the erosion distribution in the study area has verified that the accuracy rate of the erosion intensity assessment reaches 82.75%.

of the beach (T4). Using an objective independent weight method and combining geographical information technology methods with field investigation validation, the study conducts research on the intensity of coastal erosion and comprehensively assesses the coastal erosion intensity index of the Qionghai-Wanning coast in the eastern part of Hainan Island.

(1) The assessment results divide the study area into six levels: serious erosion (3.45%), strong erosion (6.90%), erosion (20.69%), micro-erosion (44.38%), stabilization (20.69%), and accretion (3.45%). Under the overall trend of global climate warming and sea-level rise, most sandy coasts are in a state of micro-erosion intensity. Strong erosion and serious erosion, influenced by human activities, often occur at capes, artificial islands, port, and other locations. Some distributions with coral reefs, beach rocks, and other geomorphic characteristics can weaken wave energy and reach a stable state, while locations with high flow estuaries may exhibit siltation due to long-term sand transport.

(2) The analysis of the correlation between various factors and the erosion intensity index reveals a significant linear relationship among the annual rate of shoreline change (T1), beach annual down-cutting rate (T2), average particle size of the beach (T4), and the coastal erosion intensity index (EII). The primary factors influencing coastal erosion intensity are the annual rate of shoreline change (T1) and the beach annual down-cutting rate (T2), while the average particle size of the beach (T4) serves as a secondary factor. This suggests that the greater the changes in the annual intertidal erosion rate and the coastline change rate, the higher the impact on coastal erosion intensity, and vice versa.

(3) The erosion intensity assessment results were verified through field surveys, and the results show that: the accuracy rate of the multi-index coastal erosion intensity assessment method reached 82.75%. The assessment method and results can provide a scientific basis for the management, protection, and restoration of coastlines.

# Data availability statement

The original contributions presented in the study are included in the article/supplementary material. Further inquiries can be directed to the corresponding authors.

## Author contributions

GF: Data curation, Investigation, Methodology, Project administration, Writing – original draft, Writing – review & editing. MH: Investigation, Supervision, Writing – original draft, Writing – review & editing. XC: Data curation, Supervision, Validation, Writing – review & editing. MF: Data curation, Project administration, Supervision, Validation, Writing – review & editing. YS: Conceptualization, Data curation, Investigation, Writing – review & editing. CW: Supervision, Validation, Writing – review & editing. HW: Supervision, Validation, Writing – review & editing. DZ: Supervision, Validation, Writing – review & editing.

## Funding

## Conflict of interest

Author XC was employed by the company Hainan Honsheen Investigation & Design Co., LTD.

The remaining authors declare that the research was conducted in the absence of any commercial or financial relationships that could be construed as a potential conflict of interest.

## Publisher's note

All claims expressed in this article are solely those of the authors and do not necessarily represent those of their affiliated organizations, or those of the publisher, the editors and the reviewers. Any product that may be evaluated in this article, or claim that may be made by its manufacturer, is not guaranteed or endorsed by the publisher.

## References

Bazzichetto, M., Sperandii, M. G., Malavasi, M., Carranza, M. L., and Acosta, A. T. R. (2020). Disentangling the effect of coastal erosion and accretion on plant communities of Mediterranean dune ecosystems. Estuarine. *Coast. Shelf. Sci.* 241, 106758. doi: 10.1016/j.ecss.2020.106758

Bolle, A., Neves, L. d., Nocker, L. D., Dastgheib, A., and Couderé, K. (2021). A methodological framework of quantifying the cost of environmental degradation driven by coastal flooding and erosion: A case study in West Africa, International. *J. Disaster. Risk Reduction. Volume.* 01, 2212–4209. doi: 10.1016/j.ijdrr.2020.102022

Boruff, B. J., Emrich, C., and Cutter, S. L. (2005). Erosion hazard vulnerability of US coastal counties. *J. Coast. Res.* 21, 932–942. doi: 10.2112/04-0172.1

Bozzeda, F., Ortega, L., Costa, L. L., Fanini, L., Barboza, C. A. M., and McLachlan A and Defeo, O. (2023). Global patterns in sandy beach erosion: unraveling the roles of anthropogenic, climatic and morphdynamic factors. *Front. Mar. Sci.* 10. doi: 10.3389/fmars.2023.1270490

Bruun, P. (1962). Sea-level rise as a cause of shore erosion. *J. Waterways. Harbours. Divisions.* 88, 117–130. doi: 10.1061/JWHEAU.0000252

Bu, Y. (2021). Research on erosion evaluation of cape and bay coasts in wenzhou area. North China University of Water Resources and Electric Power, Zhengzhou, 3–4.

Cabrera, J. S., and Lee, H. S. (2019). Flood-prone area assessment using GIS based multi-criteria analysis: A case study in davao oriental, Philippines. *Water* 11, 2203. doi: 10.3390/w11112203

Cabrera, J. S., and Lee, H. S. (2020). Flood risk assessment for davao oriental in the Philippines using geographic information system-based multi-criteria analysis and the maximum entropy model. *Flood. Risk Management.* 13, e12607. doi: 10.1111/jfr3.12607

Chao, C. (2019). *A coastal erosion intensity evaluation method based on the MABAC comprehensive algorithm.* Patent for invention, *patent number: CN202210866716.4.*

Chao, C., Cai, F., and Qi, H. s. (2022a). Coastal erosion vulnerability in mainland China based on fuzzy evaluation of cloud models. *Front. Mar. Sci.* 01. doi: 10.3389/fmars.2021.790664

Chao, C., Zhu, K., and Cai, F. (2022b). Vulnerability evolution of coastal erosion in the pearl river estuary great bay area due to the influence of human activities in the past forty years. *Front. Mar. Sci.* 03. doi: 10.3389/fmars.2022.847655

Chapman, D. M., Geary, M., Roy, P. S., and Thorn, B. G. (1982). *Coastal evolution and coastal erosion in New South Wales* (Sydney: Coastal Council of NSWSydney).

Chen, J. (2010). *Marine Resources and Environmental Conditions in Hainan Province* (Peking: China Ocean Press), 514–515.

Chen, J., Huanting, S., and Caixing, Y. (1988). *Dynamic process and geomorphological evolution of the Yangtze Estuary* (Shanghai: Shanghai Science and Technology Press).

Chen, S., Guoan, Z., Shilun, Y., and Zhiying, Y. (2004). Temporal and spatial variation of suspended sediment concentration and sediment resuspension in the

waters of the Yangtze Estuary. *Chin. J. Geogr.* 02), 260–266. Available at: https://kns.cnki.net/kcms2/article/abstract?v=VKFFl0Cm57a8oTgh_J9VsXs_L6l_KqQiyI_CR_fMpkqzhkJXa6OhxC5PgFb62XHIkbyuDqrGpGagjRZmKvFt64ACTKHLKK_DO_2pkGABgulzEgOyFX_R3xbOU8kIPg7o&uniplatform=NZKPT&language=CHS.

Cigdem, O., Perez, K., and Mayo, T. (2020). The impacts of wave energy conversion on coastal morphodynamics. *Sci. Total. Environ.* 712, 136424. doi: 10.1016/j.scitotenv.2019.136424

Dano, R., Reniers, Ad., van Dongeren, Ap., van Thiel de Vries, J., McCall, R., and Lescinski, J. (2009). Modelling storm impacts on beaches, dunes and barrier islands. *Coastal Eng.* 56, 11-12, 1133–1152. doi: 10.1016/j.coastaleng.2009.08.006

Deepika, B., Avinash, K., and Jayappa, K. S. (2013). Shoreline change rate estimation and its forecast: remote sensing, geographical information system and statistics-based approach. *Int. J. Environ. Sci. Technol.* 11 (2), 395–416. doi: 10.1007/s13762-013-0196-11-22

Dionísio, A. S., van der Werf, J., Horstman, E., Cáceres, I., Alsina, J., van der Zanden, J., et al. (2023). Influence of beach slope on morphological changes and sediment transport under irregular waves. *J. Mar. Sci. Eng.* 11, 2244. doi: 10.3390/jmse11122244

Elsayed, S. M., and Oumeraci, H. (2017). Effect of beach slope and grain-stabilization on coastal sediment transport: An attempt to overcome the erosion overestimation by X-Beach. *Coast. Eng.* 121, 179–196. doi: 10.1016/j.coastaleng.2016.12.009

Enríquez, A. R., Marcos, M., Falqués, A., and Roelvink, D. (2019). Assessing beach and dune erosion and vulnerability under sea level rise: A case study in the mediterranean sea. *Front. Mar. Sci.* 6. doi: 10.3389/fmars.2019.00004

Feng, C. (2021). "General report on the current evaluation of coastal erosion and its prevention and control technology," in *research report on the "908 Special Project"* (Peking: China Ocean Press), 1–193.

Feng, C., Cao, C., Qi, H., Su, X., Lei, G., Liu, J., et al. (2022). Rapid migration of mainland China's coastal erosion vulnerability due to anthropogenic changes. *J. Environ. Manage.* 319, 115632: 1–15. doi: 10.1016/j.jenvman.2022.115632

Feng, C., Su, X., and Cao, C. (2019). *China Coastal Erosion Vulnerability Assessment and Demonstration Application* Vol. 08 (Beijing: Ocean Press), 241–247.

Feng, C., Su, X., Liu, J., Li, B., and Lei, G. (2008). Coastal erosion problems and preventive countermeasures in my country under the background of global climate change. *Prog. Natural Sci.* 10), 1093–1103. Available at: https://kns.cnki.net/kcms2/article/abstract?v=VKFFl0Cm57a9AHtJj9eP6bSaRfw0sglkNAPgM_–6MAh8y4qx7PLRd-RItiG0Y9nG9krt6vQ0YJpqaKdxSw64Eq_jogAIdt_cs9o23DOLrhhp-O40kA8lgMXN5IvMzl&uniplatform=NZKPT&flag=copy.

Feng, A., and Xia, D. (2003). Classification of coastal erosion disasters. *Coast. Eng.* 02), 60–66. Available at: https://kns.cnki.net/kcms2/article/abstract?v=VKFFl0Cm57a0apTm9t5FJcIFiP47UOP201MxCKE04c4t1cQJGhFQOJskdkcqzh6zaxJeM31oFi2L2GiQ

SHZob0L4YFfxY_iDNxewMvIpCBwm5Bwd81klFjwZWZs4HiNm&uniplatform=
NZKPT&language=CHS.

Fu, G., Cao, C., Fu, K., Song, Y., Yuan, K., Wan, X., et al. (2022). Characteristics and evaluation of coastal erosion vulnerability of typical coast on Hainan Island. *Front. Mar. Sci.* 9. doi: 10.3389/fmars.2022.1061769

Hagedoorn, L. C., Addo, K. A., Koetse, M. J., Kinney, K., and van Beukering, P. J. H. (2021). Angry waves that eat the coast: An economic analysis of nature-based and engineering solutions to coastal erosion. *Ocean. Coast. Manage.* 11, 0964–5691. doi: 10.1016/j.ocecoaman.2021.105945

Jabour, J. (2011). Disappearing destinations: Climate change and future challenges for coastal tourism. *CABI.*

Liu, X. (2015). Coastal evolution and intrusion vulnerability assessment of abandoned yellow river delta. *Shanghai. East. China Normal. Univ.* 06, 2–4.

Ma, G.-b., Wang, W. w., Wang, Y. g., Fu, Y. b., and Yuan, L. (2017). Evaluation of the erosion status of sandy beach coast along the eastern coast of the liaodong bay from 2014 to 2015. *Coast. Eng.* 09, 36–33. doi: 10.3969/i.issn.1002-3682.2017.03.003

Mangor, K. (2017). Shoreline management guidelines (Netherlands: DHI Water and Environment), 451pp. Available at: https://www.dhigroup.com/upload/campaigns/ShorelineManagementGuidelines_Feb2017.pdf.

Marcel, M. (2012). Concepts and science for coastal erosion management: for policy makers R/Ol (2012-09-24)[2017-05-31]. Available at: http://hdl.handle.net/1969.3128859.

McFall, B. C. (2019). The relationship between beach grain size and intertidal beach face slope. *J. Coast. Res.* 35, 1080–1086. *Coconut Creek (Florida),* ISSN 0749-0208. doi: 10.2112/JCOASTRES-D-19-00004.1

Merlotto, A., B´ertola, G. R., and Piccolo, M. C. (2016). Hazard, vulnerability and coastal erosion risk assessment in necochea municipality, buenos aires province, Argentina. *J. Coast. Conserv.* 20, 351–362. doi: 10.1007/s11852-016-0447-7

Mohamed, E.-S. E.-M., Ali, S. S., Fawzia, E. M., Abbas, S., and Naglaa, S. (2021). Coastal erosion risk assessment and applied mitigation measures at Ezbet Elborg village, Egyptian delta. *Ain. Shams. Eng. J.* 13, 10. doi: 10.1016/j.asej.2021.10.016

Mosadeghi, R., Warnken, J., Tomlinson, R., and Mirfenderesk, H. (2015). Comparison of FuzzyAHP and AHP in a spatial multi-criteria decision making model for urban land-use planning. *Comput. Environ. Urban. Syst.* 49, 54–65. doi: 10.1016/j.compenvurbsys.2014.10.001

Nan, X., and Gong, P. (2018). Significant coastline changes in China during 1991-2015 tracked by Landsat data. *Sci. Bull.* 63, 883–886. doi: 10.1016/j.scib.2018.05.032

Nans, B., Ronadh, C., and Masselink, G. (2019). From fine sand to boulders: Examining the relationship between beach-face slope and sediment size. *Mar. Geol.* 417. doi: 10.1016/j.margeo.2019.106012

Rodgers, J. L., and Nicewander, W. A. (1988). Thirteen ways to look at the correlation coefficient. *Am. Statis. tician.* 42, 59–64. doi: 10.1080/00031305.1988.10475524

Saffaria, S., Mahmoudi, A., Shafiee, M., Jasemi, M., and Hashemi, L. (2020). Measuring the effectiveness of AHP and fuzzy AHP models in environmental risk assessment of a gas power plant. *Hum. Ecol. Risk Assess.* 27, 1227–1238. doi: 10.1080/10807039.2020.1816809

Senevirathna, E. M. T. K., Edirisooriya, K. V. D., Uluwaduge, S. P., and Wijerathna, K. B. C. A. (2018). Analysis of causes and effects of coastal erosion and environmental degradation in southern coastal belt of Sri Lanka special reference to unawatuna coastal area. *Proc. Eng.* 212, 1010–1017. doi: 10.1016/j.proeng.2018.01.130

Shao, C. (2016). Study on coastal erosion and adaptive management of beachcoral reef (Xiamen: Third Institute Oceanography State Oceanic Administration), 50–63. Available at: https://kns.cnki.net/KCMS/detail/detail.aspx?dbname=CMFD201701&filename=1016256149.nh.

Shi, P., and Kasperson, R. (2015). World atlas of natural disaster risk. *Springer-Verlag. Berlin.* 61, 534–536. doi: 10.1111/1745-5871.12615

Shi, L., Li, J., Dong, P., Ying, M., Li, W., and Chen, S. (2007). An experiment study of erosion characteristics of sediment bed at the yellow river delta. *Coast. Eng. J.* 49, 25–43. doi: 10.1142/S0578563407001526

Shuai, J., Xu, N., Li, Z., and Huang, C. (2021). Satellite derived coastal reclamation expansion in China since the 21st century. *Global Ecol. Conserv.* 30. doi: 10.1016/j.gecco.2021.e01797

Shuying, Z., Hu, Y., and Xing, S. (2018). Water source identification of water inburst based on independence weight and grey correlation degree theory. *Hydrogeol. Eng. Geol.* 45, 36–41 + 62. doi: 10.16030/j.cnki.issn.1000-3665.2018.06.06

Thampanya, U., Vermaat, J. E., and Sinsakul, S. (2006). Coastal erosion and mangrove progradation of Southern Thailand. *Estuarine. Coast. Shelf. Sci.* 68, 75–85. doi: 10.1016/j.ecss.2006.01.011

The SPSSAU Project (2024). SPSSAU. (Version 24.0) Available online at: https://www.spssau.com. (accessed May, 2024).

Tim, S., Masselink, G., and Russell, P. (2011). Morphodynamic characteristics and classification of beaches in England and Wales. *Mar. Geol.* 286, 1–20. doi: 10.1016/j.margeo.2011.04.004

Wen, S. Y., Zhang, F. S., Wang, X., Wang, X. X., Li, F., Wang, F., et al. (2017). "Risk assessment method of coastal erosion disasters," in *7th Annual Meeting of Risk-Analysis-Council of China-Association-for-Disaster-Prevention, 01-18,* Vol. 128). 38–42. Available at: https://webofscience.clarivate.cn/wos/woscc/full-record/WOS:000390886700006.

Xia, D., Wang, W., and Wu, G. (1993). Coastal erosion in China. *Acta Geographica. Sin.* 48, 468–475. Available at: https://kns.cnki.net/kcms2/article/abstract?v=VKFFl0Cm57YVFrQGC-6b6SVcpmlQhOxhtXmEnaIJPdW6YwABahU5wysbzuw_9ZzkFOM0fwmrDSmUFx0awQKk5UAcY8EpFCpxCjmpJHwILbNhvCEFO5q6xy5N7SF07rof&uniplatform=NZKPT&language=CHS.

Zhou, J., and Ma, S. (2024). *SPSSAU Research Data Analysis Methods and Applications. 1st Edition* (Peking: Electronic Industry Press), p. 59–99.